Design and Analysis of High-Bypass Turbofan Engine Nacelle to Enhance Performance

Mouhamadou M. Diop[1] and Adeel Khalid[2]
Kennesaw State University, Marietta, GA 30060, U.S.A.

The CFM56-7B, a high-bypass turbofan engine developed by CFM International in collaboration with General Electric and Safran Aircraft Engines, represents a cornerstone in modern aviation propulsion, extensively powering aircraft models like the Airbus A320, Boeing 737 NG, and Embraer E-Jet families. The objective of the research is to identify opportunities to enhance the performance and efficiency of the CFM56-7B engine. With the intention of modifying the nacelle's profile to increase pressure inside the inlet, an examination of wind speeds and pressure on the CFM56-7B engine's inlet is presented. The efficiency and performance of the engine can be increased by optimizing the airflow through the nacelle, which can result in less fuel being used and fewer pollutants expelled. The size and shape of the nacelle are modified in this research. The goal is to determine the optimal combination of these parameters that will help optimize the air pressure before the compressor. This will help increase inlet and compressor efficiency and overall engine performance.

I. Nomenclature

A	=	Angle of attack of Upper Airfoil (A)
δ	=	Percentage drag reduction
Δ_{Drag}	=	Average drag force
L	=	Inlet Lower Length (L)
P/V_{ratio}	=	Average velocity / Average pressure ratio
R	=	Wind speed evaluation distance
U	=	Inlet Upper Length
V	=	Vertical Diameter

II. Introduction

The aviation industry is grappling with multifaceted challenges, including those related to environmental sustainability, rising fuel costs, and higher competitiveness. Continuous improvements in aircraft and engine economy are essential to meet these challenges. Optimization is a gradual and continuous process for engineers in civil aviation. Several studies have been conducted on existing aircraft engines to analyze performance. Yilmaz [1] presented a study that relates exhaust gas temperature (EGT) and engine operational parameters in CFM56-7B engines where they concluded that the relationship between EGT and the majority of the operational parameters of the engine is not strong in the studied turbofan engine. Cilgin & Turan [2] conclude that efficiency of the turbofan is determined to be 14 %, while propulsive and thermal efficiencies of the turbofan are 35 % and 40 %, respectively. Analysis on turbofan engines can be limited by factors like accurate modeling using CAD (Computer Aided Design) approach. In the context of engine performance enhancement, utilization of CAD models to reduce air velocity and increase air pressure inside the inlet of the engine is the preferred route. Simplifying assumptions are made in the creation of CAD models of the CMF56-7B.

[1] Undergraduate, Mechanical Engineering, College of Engineering and Engineering Technology, and AIAA Student Member (Membership Number: 1550910).
[2] Interim Assistant Dean of Research, College of Engineering and Engineering Technology, and AIAA Member.

Once models are created, Computational Fluid Dynamics (CFD) is used to investigate wind speeds, pressure, lift and drag on a turbofan engine 3D model. The procedures include a 2D to 3D analysis of the air flow inside the inlet. They were conducted using the SOLIDWORKS Flow Simulation. This approach is evolutionary. Once the engineering CAD models of this engine are created, new data can be obtained for various geometries without changing the domain, mesh, and boundary conditions.

III. Design

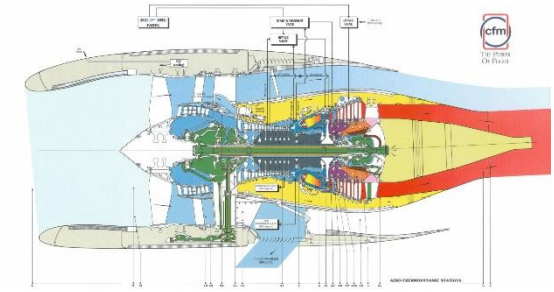

Fig. 1 Cross section of CFM56-7B [8].

Fig. 2 Front view of the CFM56-7B [7].

The designs in this study include a baseline model, twenty-four iterations of geometries and an "optimized" model. The baseline model is created using a cross section of the CFM56-7B in SOLIDWORKS as shown in **Fig. 1**. Traces of the cross section constitute the front plane of the baseline. **Fig. 2** shows the front of a CFM56-7B and represents the right plane of the baseline. This method provides a sketch of the longitudinal and frontal features of the engine. The main challenge for this design is to produce an accurate model that conforms to the dimension ratios of the engine, attention is directed to the geometry of the nacelle. Auxiliary features outside the nacelle (gears, fan, compressors, combustion chamber, turbines, and their blades) are not included in this study (**Fig. 3**).

Fig. 3 CFM56-7B Baseline model 3D sketch.

Iterative models are configurations of the baseline where one of the following parameters is modified: inlet upper length, inlet lower length, inlet diameter and upper airfoil angle of attack. Each parameter is modified (increased and reduced) following the design matrix shown in **Table 1**. There are twenty-four models in total for each configuration (parameter changes). These parameters are shown in **Fig. 4**.

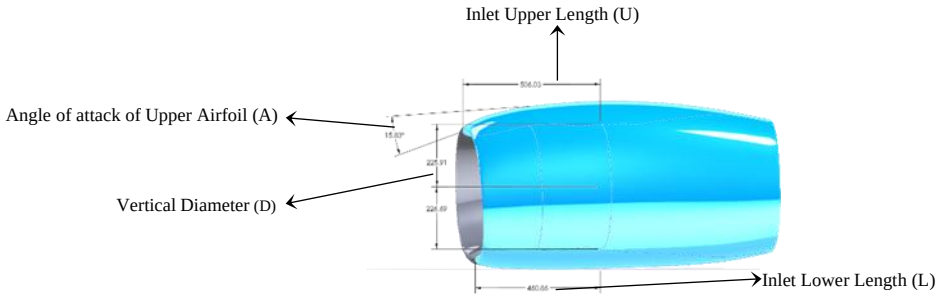

Fig. 4 Parameters subjected to modifications.

The "Optimized" model is developed based on the analysis of the results. The best iteration for each parameter is selected and incorporated into a new model that would represent the optimum configuration of the CFM56-7B (**Fig. 5**).

Fig. 5 CFM56-7B "Optimized" model 3D sketch.

To register wind speeds during computation, a sketch of a reference line is added from the interior to the inlet to the tip of the nose cone, as shown in **Fig. 6**. The wind speed is registered along this reference line. Measurements are made along this line and shown in figures 10, 11, 12,13 and 15. The line starts at the tip of the nose cone (labeled as 0 m) and extends to the middle of the inlet (0.5 m).

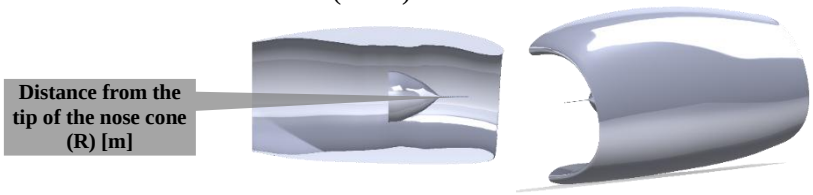

Fig. 6 Wind speed evaluation distance (R).

The engine models are ultimately scaled uniformly about the origin by a factor of 4.041 to replicate the actual dimensions of a CFM56-7B as closely as possible. Information about the dimensions of the CFM56-7B are published by the European Union Aviation Safety Agency [3].

Table 1. Parameter matrix for CFM56-7B design iterations

Variable	-5%	-2.5%	-1.0%	Baseline (mm)	1.0%	2.5%	5.0%
Inlet upper length (U)	480.73	493.38	500.97	506.03	511.09	518.68	531.33
Inlet lower length (L)	437.82	449.34	456.25	460.86	465.47	472.38	483.90
Inlet diameter (D)	429.97	441.28	448.07	452.60	457.12	463.91	475.23

Variable	-10.0%	-5.0%	-2.5%	Baseline (deg)	2.5%	5.0%	10.0%
Angle of Attack (A)	14.25	15.04	15.44	15.83	16.23	16.63	17.42

IV. Computation

Computational Fluid Dynamics (CFD) analysis is performed to measure the impact of the above stated design iterations on the nacelle efficiency. CFD is commonly used in the aerospace industry for similar analyses [4].

A. Goals

Wind speeds inside the inlet of the 3D model of the engine are calculated using SOLIDWORKS Flow Simulation (SWFS). Uniformity of the boundary conditions and in mesh generation are crucial in the analysis. The computation compares the velocity and pressure of the air inside the inlet between the baseline and iterative models. The goal of modifying the nacelle geometry is to reduce air speed and increase pressure inside the inlet. Therefore, this study uses P/V_{ratio} (average pressure divided by average velocity) as a metric that will simplify qualitative analysis.

P/V_{ratio} , in addition to the individual values of average velocity or average pressure, is utilized to determine the design modifications in each parameter. Solitary use of P/V_{ratio} may lead to incomplete results. If P/V_{ratio} for different configurations are numerically close, the method suggests a review of each metric followed by a selection of the P/V_{ratio} with the lowest average velocity or the highest average pressure.

The velocity and pressure values are reported on a XY plot, and averages are calculated.

B. Boundary Conditions

This project is developed using the System International metric system (m·kg·s). Analysis type is External Fluid Flow with an exclusion of cavities without conditions. Default fluid is air characterized by a Laminar and Turbulent type. Initial and ambient conditions replicate commercial flight cruise conditions at velocity directed in the X-direction towards the engine inlet [5].

C. Computational Domain

A 3-dimensional domain is set around the engine where the Z-axis is symmetrical. The CFM56-7B symmetry around the front plane is utilized to reduce the usage of computer resources. Each calculation in the domain is thus duplicated symmetrically towards the other half of the engine model.

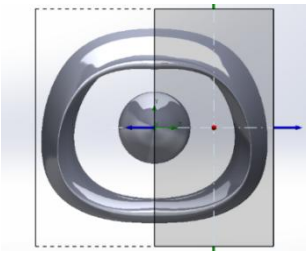

Fig. 7 Computational domain in SOLIDWORKS Flow Simulation.

D. Mesh Generation

Mesh generation is one of the most crucial steps when performing simulation procedures in CFD. Flow Simulation computational approach is based on locally refined rectangular mesh near geometry boundaries [6]. A basic quadrilateral structured mesh is generated using default parameters (Level 3) as global mesh. The global mesh separates the computational domain into slices but will not provide the accuracy desired during simulation. Mesh refinement is therefore introduced.

The computational domain containing rectangular computational mesh cells is split into eight cells by three orthogonal planes that divide the edge of the cells into halves. This procedure uses Solution-Adaptive Refinement (SAR). The Refinement level specifies how many times the initial mesh cells can be split to achieve the solution-adaptive refinement criteria and therefore manages the minimum computational mesh cell size. By using Equidistant Refinement option, specified settings are used to refine the cells within the region bounded by surfaces equidistant from the selected objects [6].

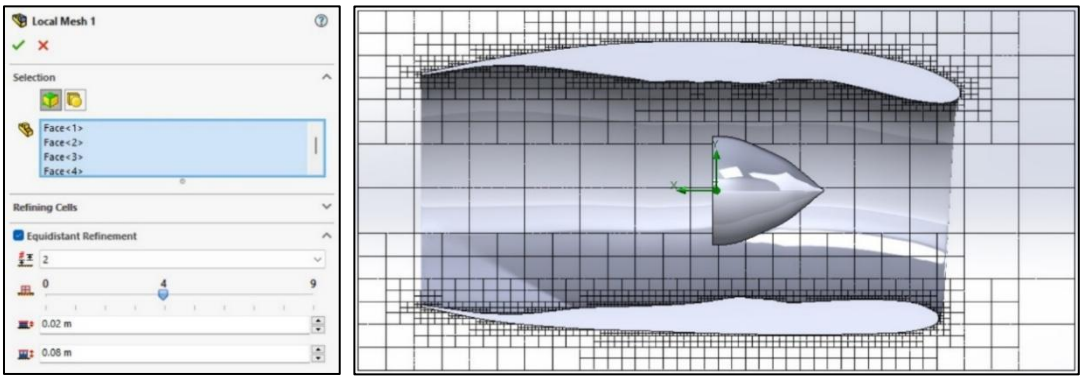

Fig. 8 Local mesh definition and local mesh cut plot around the CFM56-7B baseline model.

V.Results

A. Baseline

3-dimensional CFD simulations are conducted in SWFS to include the whole engine. The domain includes half of the engine however the results are extrapolated using symmetry about the front plane. Simulation is run without a set number of iterations; data is collected upon convergence [6]. Percentage difference for average velocity and average pressure between the baseline and "optimized" model is calculated.

The value of the average velocity inside the inlet is recorded at 507.30 Km/h while the average value of the pressure is recorded at 32516 Pa. P/V_{ratio} for the baseline is estimated at 64.1.

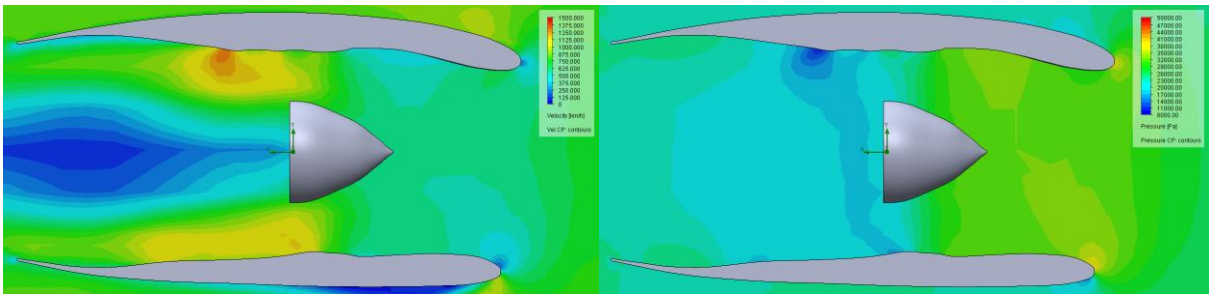

(a) (b)

Fig. 9 Velocity (a) cut plot and pressure (b) cut plot for engine baseline model.

B. Iterations

Following the design matrix in Table 1, 3-dimensional CFD simulations are conducted for the 6 upper inlet length iterated models, 6 lower inlet length iterated models, 6 diameter length iterated models and 6 angle of attack of the engine's upper airfoil iterated model using the same computation procedure for each.

1. Inlet length iterations

Average velocity and average pressure values are estimated using the XY-Plots. It is observed that the average velocity inside the inlet reaches its minimal value of 455.34 Km/h for the model with a reduction of the inlet upper length of 5% compared to the other configurations. Similarly, the average pressure also reaches its maximal value of 33750 Pa for the engine model with a reduction of the inlet upper length of 5%. P/V_{ratio} comparison confirms the overall observations (a reduction of the inlet upper length by 5% offers a ratio of 74.1 which is higher than the baseline and all other configurations).

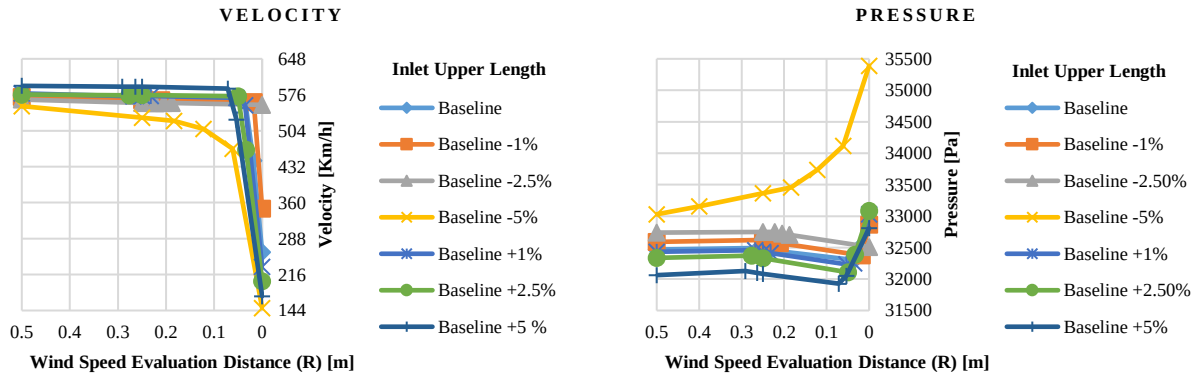

Fig. 10 Average velocity and average pressure comparison inside inlet (U iterations).

The statistical analysis regarding the average velocity and pressure inside the inlet reveals that average velocity reaches its minimal value of 502.99 Km/h with the inlet lower length is increased by 5% compared to the other configurations. Similarly, the average pressure also reaches its maximal value of 32745 Pa for the engine model with an augmentation of the inlet lower length of 5%. P/V_{ratio} comparison confirms the overall observations (an augmentation of the inlet lower length by 5% offers a ratio of 65.1 which is higher than the baseline and the other configurations).

It is important to note that the inlet lower length variations have a marginal effect on the velocity changes.

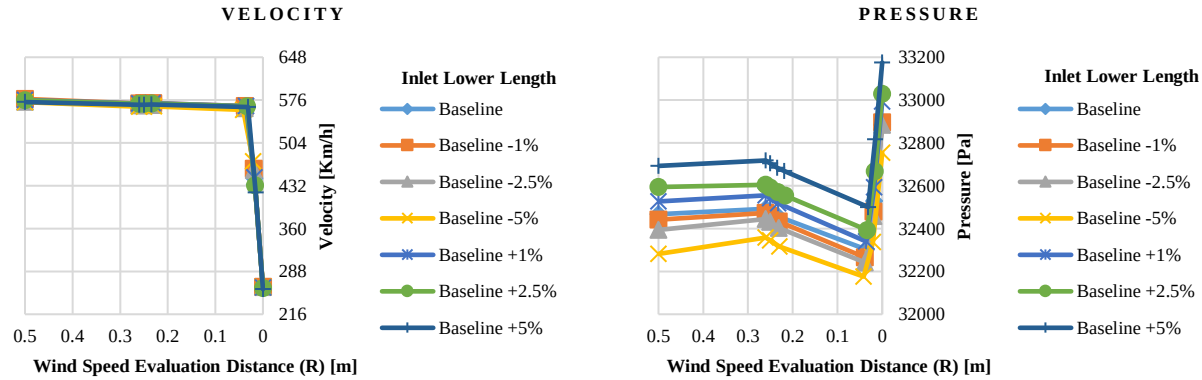

Fig. 11 Average velocity and average pressure comparison inside inlet (L iterations).

2. Vertical diameter iterations

Average velocity and average pressure are estimated using XY-Plots comparably to the previous section. Observations show that average velocity inside the inlet reaches its minimal value of 417.92 Km/h for the

configuration where the diameter of the engine is reduced by 5% compared to the other configurations. In parallel, the average pressure also reaches its maximal value of 33047 Pa for the engine model where the diameter of the engine is reduced by 5%. P/Vratio comparison confirms the overall observations (a 5% reduction of the vertical diameter offers a ratio of 79.1 which is higher than the baseline and the other configurations).

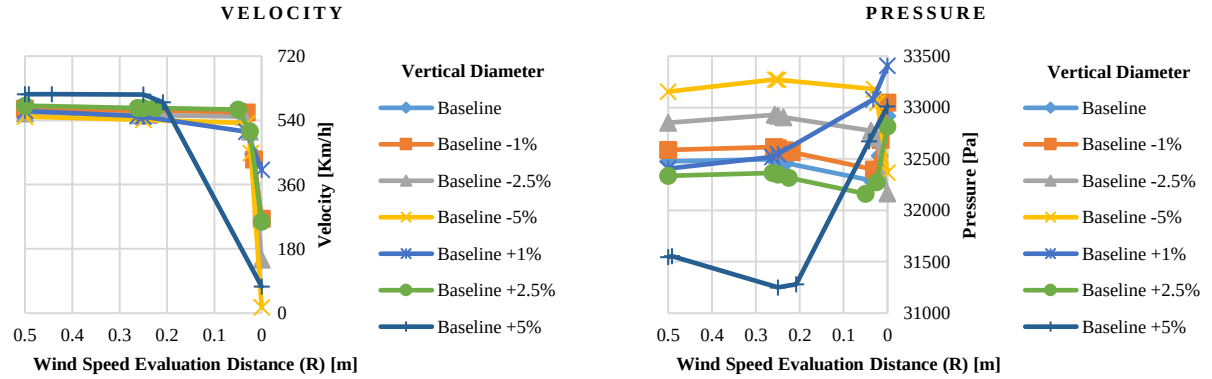

Fig. 12 Average velocity and average pressure comparison inside inlet (D iterations).

3. Angle of attack of upper airfoil iterations

Average velocity inside the inlet reaches its minimum value of 507.03 Km/h for the configuration where the angle of interest is reduced by 5% compared to the other configurations. However, the average pressure reaches its maximal value of 32523 Pa for the engine model. P/Vratio comparison reveals that a 10% reduction of the vertical diameter offers a ratio of 64.3. The difference in P/Vratio is marginal when it comes to the angle changes. It can be explained by the fact that the minimal velocity is very mildly affected by these modifications and is therefore marginal. Overall, the best iteration selected is the configuration where the angle is reduced by 10% because the average pressure is higher for this setup.

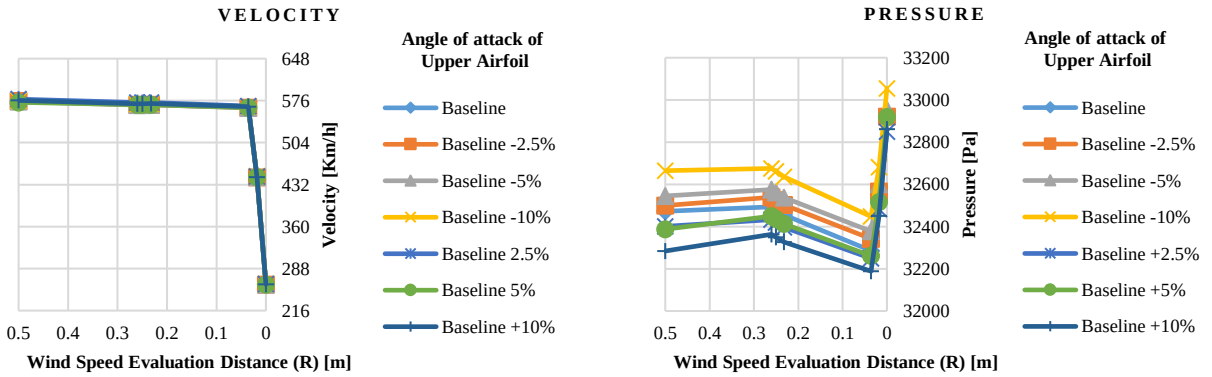

Fig. 13 Average velocity and average pressure comparison inside inlet (A iterations).

Table 2. P/V$_{ratio}$ for design iterations of CFM56-7B

Variable	-5.0%	-2.5%	-1.0%	Baseline	1.0%	2.5%	5.0%
Inlet upper length (U)	74.1	58.4	61.6	64.1	62.2	65.5	61.5
Inlet lower length (L)	63.6	63.9	63.6	64.1	64.1	64.5	65.1
Inlet diameter (D)	79.1	66.8	64.7	64.1	63.6	62.3	61.3

Variable	-10.0%	-5.0%	-2.5%	Baseline	2.5%	5.0%	10.0%
Angle of Attack (A)	64.3	64.3	64.2	64.1	63.6	64.1	63.7

4. "Optimized" model

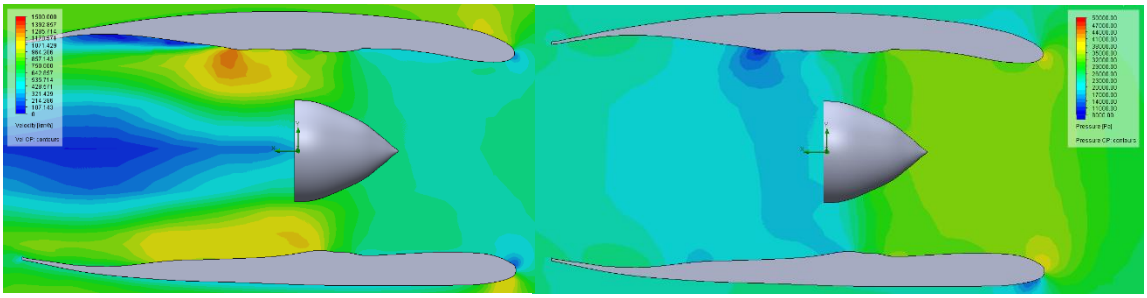

(a) (b)

Fig. 14 Velocity (a) cut plot and pressure (b) cut plot for engine "optimized"

Following the discoveries and conclusions of the 25 CFD simulations of the baseline and iterative engines, an additional model incorporating the best modifications leading to maximal pressure - minimal velocity is sketched. CFD simulations on the iterated models suggested that a reduction of the inlet upper length of 5%, an augmentation of the inlet lower length by 5%, a 5% reduction of the vertical diameter and a 10% reduction of the upper airfoil angle of attack on the CFM56-7B baseline 3D model would yield desired outcomes for average velocity and average pressure. Following that data, an "optimized" model is sketched by implementing the mentioned changes on the baseline model.

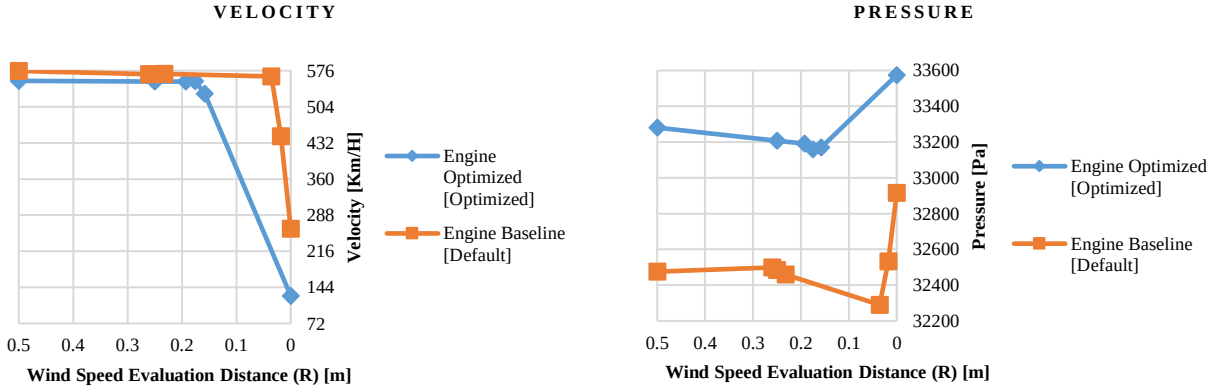

Fig. 15 Average velocity and average pressure comparison between baseline model and "optimized" model.

CFD simulation is ran following the standard procedure of the study on the "optimized" model. The optimized model shows improvements compared to the baseline, offering lower velocity average and higher pressure build up. The data collected reveals that the average velocity inside the inlet is evaluated at 479.29 Km/h and the average pressure reaches 33264 Pa. The percentage difference between the baseline and optimized model is 5.68% for velocity and 2.27% for pressure inside the inlet.

VI. Experimental Procedure

A. Introduction

Results obtained after the CFD analysis and data collection have shown a trend with a reduction in air velocity and an augmentation in pressure inside the inlet of the optimized engine model. A wind tunnel experiment is designed with the objective of validating CFD results.

B. Experiment Setup

Fig. 16 AEROLAB Educational Wind Tunnel EWT used for data collection

The AEROLAB Educational Wind Tunnel (EWT) is of the Eiffel, or Open Circuit, type with a 12"x12"x24" (30.48cm x 30.48cm x 60.96cm) test section. The tunnel is equipped with an aluminum honeycomb flow straightener and two turbulence-reducing screens. The testing section is equipped with a sting balance that is mounted on the plate and is used to change the angle of attack of the model (**Fig. 17**).

Fig. 17 Balancing Sting inside the test section.

The EWT comes with a computer application that both controls and displays data. The description of the display is as follows:

Normal Force – Displays the Normal Force (Lift) exerted on the balance.
Axial Force – Displays the Axial Force (Drag) exerted on the balance.
Pitching Moment – Displays the Pitching Moment (or Yawing Moment depending on the balance orientation) being placed on the balance.

For the Experiment, SI units will be utilized for data collection and the Speed Control (air speed) will not exceed 50%.

Fig. 18 EWT computer application.

C. 3D Model design changes for the experiment

Changes are made to the 3D models to facilitate the completion of the experimental procedure. The nose cone inside the 3D models is attached to the inner sides of the models by two aerodynamic shafts that form a cross. In addition to that, a protrusion is added to the back of the cone and will be coupled with a mounting pin tailored to the balancing sting of the wind tunnel. The pistons are created close to the base of the nose cone to avoid any interference with the wind entering the nacelle.

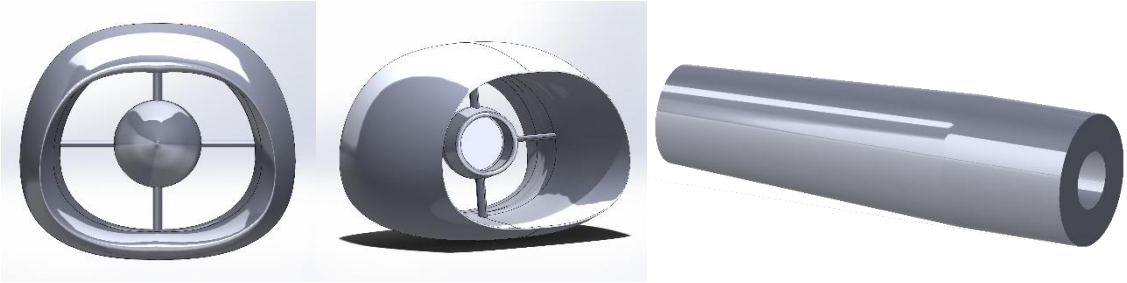

Fig. 19 Implemented changes for 3D prints and mounting pin.

D. 3D Printing

The 3D printing process is started by exporting the 3D models into the slicer software *GrabCAD Print.* To do so, the SolidWorks Part file is directly opened into the slicer. After placing the models in the virtual tray, the infill values for both drawings are set to 30% in the model settings. All other parameters remain as default and the print job is exported to the Stratasys F170 printer. The print is completed with F123 ABS material and F123 QSR support. The mounting pin is printed using Dremel 3D45 printer. The model of the pin is loaded into *Digilab 3D Slicer*. The material selected for this job is PLA and the profile is Medium Quality (0.2mm). All other parameters are set to default, and the print job is exported to the Stratasys F170.

E. Procedure

Following the preparation, the Baseline Model Experiment is conducted. The baseline model is placed in the wind tunnel and the pitch angle is set to 0 degrees. The experiment starts with an air speed of 10%. The axial force and normal force are recorded. The air speed is increased in increments of 10%, with the drag being recorded at each increment. This process is repeated for pitch angles of -15, -10, -5, +5, +10, and +15 degrees, respectively. After the completion of the baseline model experiment, the Optimized model experiment is conducted. The same steps are repeated with the optimized model. Finally, the Data Reduction phase takes place. The Normal Force and Axial Force are converted to Lift and Drag components using the following formula:

$$Drag = N \sin\alpha + A \cos\alpha$$

where α represents the angle of attack, N represents the Normal Force, and A represents the Axial Force. The drag recorded for the baseline and optimized models at different air speeds and pitch angles is compared. The performance of the two models is analyzed based on the recorded data. This concludes the procedure.

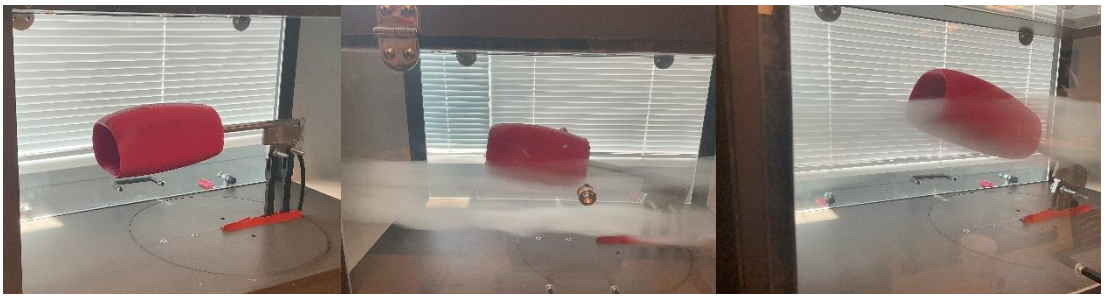

Fig. 20 Baseline model during the experiment.

F. Experiment Results

Drag calculated using the formula provided in the procedure shows that there is a slight difference in the amount of drag force experienced by the optimized model in comparison to the baseline model. The quantity Δ_{Drag} represents the difference in drag between the baseline engine model at a pitch angle of 0° and each configuration. The behavior of the engine at various angles of attack is reasonably similar with slight value differences for drag experienced as depicted in the **Fig. 21**.

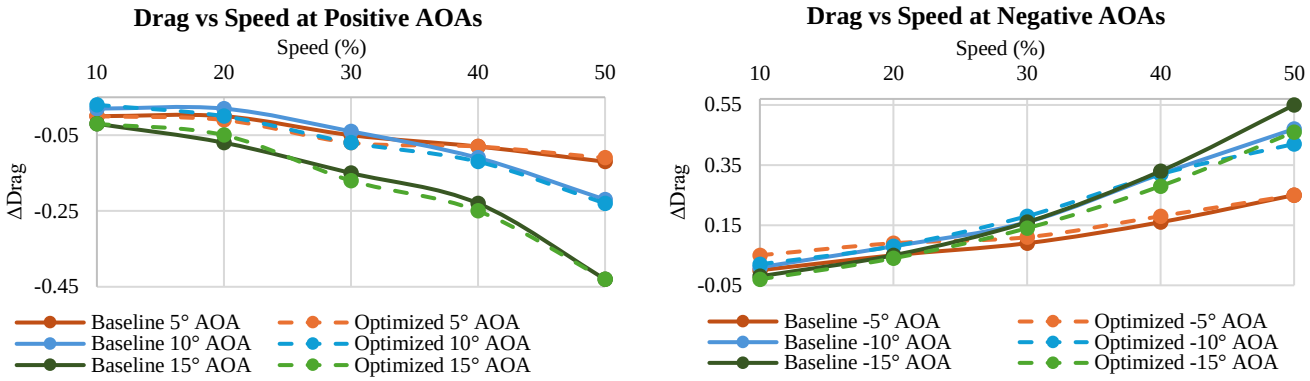

Fig. 21 Variation of the Drag Force with Wind Speed at Positive and Negative Angles of Attack.

Following these results, it is reasonable to assume that the optimized model experiences less drag than the baseline, and that, therefore, the dimensions changes will result in an engine with higher pressure and lower velocity inside the inlet. The percentage drag reduction noted δ evaluates the reduction of the average drag force experienced by the optimized model at the configuration angles and is calculated as follows:

$$\delta = \frac{\text{Avg } \Delta_{\text{Drag Optimized}} - \text{Avg } \Delta_{\text{Drag Baseline}}}{\left(\frac{\text{Avg } \Delta_{\text{Drag Optimized}} + \text{Avg } \Delta_{\text{Drag Baseline}}}{2}\right)} * 100$$

Table 3. Percentage Drag Reduction δ at the various angles of attack

Configuration	Percentage Drag Reduction δ (%)
-15° Angle of Attack	-18.37
-10° Angle of Attack	-1.94
-5° Angle of Attack	21.14
+5° Angle of Attack	-7.69
+10° Angle of Attack	-16.67
+15° Angle of Attack	-2.20

At the -5° angle of attack, the optimized model is subjected to a higher drag force compared to the baseline model. Besides that, it is observed that the Δ_{Drag} is reduced for five out of the six other studied with the highest reduction happening at an angle of 15° below horizontal.

VII. Conclusion

A 3D CAD model of the CFM56-7B is designed in SOLIDWORKS, based on the data available in the public domain. That baseline model is then iteratively modified following a design matrix that varies the lengths of the inlet (upper and lower), the diameter and the angle of the upper airfoil of the engine. A CFD simulation procedure is utilized in SOLIDWORKS Flow Simulation with the goal of analyzing the velocities and pressure inside the nacelle in cruise conditions. The data gathered suggested that a reduction of the inlet upper length of 5%, an augmentation of the inlet lower length by 5%, a 5% reduction of the vertical diameter and a 10% reduction of the upper airfoil angle of attack on the CFM56-7B baseline 3D model would yield desired outcomes for minimum average velocity and maximum average pressure inside the inlet. As those separate findings are implemented simultaneously on the "optimized" model, CFD shows that the "optimized" model offers a 5.68% decrease of the average velocity and a 2.27% increase in pressure. The experiment conducted in the wind tunnel has shown that the drag experienced by the optimized model is less than the drag experienced by the baseline at five out of six angles of attack studied. This study shows that slight modifications in the geometry of the nacelle could result in improvement in engine performance, which could therefore result in less fuel consumption and fewer harmful gases emitted into the atmosphere.

References

[1] I. Yilmaz, "Evaluation of the relationship between exhaust gas temperature and operational parameters in CFM56-7B engines," *Proceedings of the Institution of Mechanical Engineers, Part G: Journal of Aerospace Engineering,* vol. 223, no. 4, pp. 433-440, April 2009.

[2] M. E. Cilgin and O. Turan, "Entropy Generation Calculation of a Turbofan Engine: A Case of CFM56-7B," *International Journal of Turbo & Jet-Engines,* vol. 35, no. 3, pp. 217-227, 2018.

[3] EASA, "TYPE-CERTIFICATE DATA SHEET," EASA, 2019. [Online]. Available: https://www.easa.europa.eu/en/downloads/7795/en. [Accessed 2024].

[4] L. W. Howerton and J. W. Slater, "Auxiliary Inlet Design Study for Mach 1.4," in *AIAA Propulsion and Energy 2021 Forum*, Virtual Event, 2021.

[5] E. Chu, D. Gorinevsky and S. Boyd, "Detecting Aircraft Performance Anomalies from Cruise Flight Data," in *AIAA Infotech @ Aerospace 2010,* Atlanta, Georgia, 2010.

[6] D. Systemes, *Technical Reference SOLIDWORKS Flow Simulation 2021,* 2021.

[7] "CFM56-7B SAC Engine Airflow," dokument.tips, [Online]. Available: dokumen.tips. https://dokumen.tips/documents/cfm56-7b-sac-engine-airflow.html?page=1. [Accessed 18 January 2024].

[8] Wikipedia, "CFM International CFM56," 14 January 2024. [Online]. Available: https://en.wikipedia.org/wiki/CFM_International_CFM56#/media/File:Boeing_737-400_Engine.JPG. [Accessed 18 January 2024].